

# The role of exchange interactions in superradiant phenomena

João Pedro Mendonça,<sup>1,\*</sup> Krzysztof Jachymski,<sup>1,†</sup> and Yao Wang<sup>2,‡</sup>

<sup>1</sup>*Faculty of Physics, University of Warsaw, Pasteura 5, 02-093 Warsaw, Poland*

<sup>2</sup>*Department of Chemistry, Emory University, Atlanta, Georgia 30322, USA*

(Dated: March 10, 2025)

The Dicke model is a central platform for exploring strong light-matter interaction and its superradiant properties, with implications for emerging quantum technologies. Recognizing that realistic qubits inherently experience direct interactions, we investigate the influence of both isotropic and anisotropic spin-spin couplings on the Dicke paradigm. In the strong coupling regime—where large photon populations challenge conventional numerical techniques—we developed a hybrid numerical method tailored for this problem, which demonstrates high accuracy and rapid convergence in reproducing established Dicke model results. Furthermore, our study reveals that distinct ferromagnetic and antiferromagnetic regions exhibit different orders of phase transitions. Most notably, in the presence of anisotropic interactions, we identify a novel phase where spin order and superradiance coexist, marked by enhanced superradiance with a photon number significantly exceeding that of the conventional Dicke model.

*Introduction.* Highly correlated quantum many-body systems lay the foundation for implementing quantum technologies, which exploit nonclassical correlations for computing, simulation, communication, and sensing purposes [1]. However, quantum state engineering with the desired level of accuracy remains a highly non-trivial task. Optical methods are natural candidates for realizing state preparation and quantum control schemes in various systems, owing to the availability of tunable laser light, single-photon sources, and pulse modulation techniques that allow for excellent time resolution. It is also worthwhile to consider the backaction of the system in the light field, an essential aspect for applications such as energy storage and extraction in a quantum battery [2] or state readout from quantum memories [3]. Coupling to photons can also fundamentally alter the properties of many-body systems, for instance by inducing transient superconductivity [4] or mediating long-range interactions leading to self-organization [5].

The Dicke model is a cornerstone for understanding collective interactions between a single-mode light field and matter. It has been experimentally realized in diverse platforms, including solid-state cavity QED [6], trapped ions [7], organic molecules [8], and cold gases [5, 9–11]. Central to its appeal is the superradiant phase transition, where macroscopic photon occupancy emerges as a distinctive characteristic of collective quantum behavior. Variations of this model have proven vital in understanding phenomena such as quantum batteries [12–14], polaritonic chemistry [15], and quantum spin glasses [16, 17]. In particular, photon-mediated long-range spin-spin interactions achieved via coupling to light enabled applications in quantum state engineering and spin squeezing [18–20]. However, spin-spin interactions, arising from electronic Coulomb interactions or atomic interactions, are often unavoidable in realistic material and atomic systems. These interactions are expected to significantly affect the properties of the system, deviat-

ing from the conventional Dicke model, but are usually not included into theoretical studies due to the extremely increasing complexity.

Specifically, the conventional Dicke model is represented by the Hamiltonian:

$$\begin{aligned} \mathcal{H}_{\text{Dicke}} &= \omega \left( a^\dagger a + \frac{1}{2} \right) + \frac{\varepsilon}{2} \sum_{i=1}^N \sigma_i^z + \frac{g}{\sqrt{N}} \sum_{i=1}^N \sigma_i^x (a + a^\dagger) \\ &\equiv \frac{\omega}{2} (x^2 + p^2) + \varepsilon s^z + g' s^x x, \end{aligned} \quad (1)$$

where the state of each two-level qubit is encoded by a local spin operator  $s_n^\alpha = \sigma_n^\alpha/2$ , and the photonic operators  $x = (a^\dagger + a)/\sqrt{2}$ ,  $p = i(a^\dagger - a)/\sqrt{2}$ , with  $a(a^\dagger)$  being the photon annihilation(creation) operator. Here,  $\omega$  is the cavity frequency,  $\varepsilon$  the atomic transition frequency, set to  $\omega = \varepsilon = 1$ ,  $g$  is the collective coupling strength,  $g' = 2g/\sqrt{N/2}$  accounts for the mode volume, and  $N$  is the number of atoms. The Dicke model can be mapped to an  $SU(N)$  spin model and solved exactly [21], and exhibits a phase transition between superradiant and normal phases. In this work, however, short-range Coulomb interactions between atoms are not neglected in the second quantization, leading to nearest-neighbor Heisenberg spin-spin interactions, which are unavoidable in reality. This generalization can be described by the Dicke-Heisenberg Hamiltonian, which is given by the combination of the two paradigmatic models for the spin-photon and spin-spin interactions [see Fig.1] and can be written as

$$\mathcal{H}_{\text{Dicke-Heisenberg}} = \mathcal{H}_{\text{Dicke}} - \sum_{\langle i,j \rangle} \sum_{\alpha=x,y,z} J_\alpha s_i^{(\alpha)} \cdot s_j^{(\alpha)}, \quad (2)$$

For simplicity, we consider the situation where all qubits are aligned in a 1D chain, while the method we will introduce is applicable to general systems. Our study focus on two variants of this model, which we call Dicke-Ising and Dicke-XXZ. The Dicke-Ising model considers only inter-

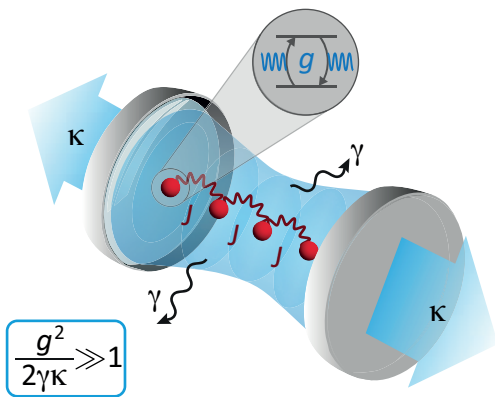


FIG. 1. Cartoon representation of the considered model. The system is composed of an ensemble of two-level quantum systems (TLSs) in an optical cavity. They can anisotropically interact with their nearest-neighbors with an exchange rate  $\mathbf{J}$ . Each TLS has a separation  $\varepsilon$  between the two states and is interacting with the cavity field with a interaction strength  $g$ . The decoherence effects  $\kappa$  and  $\gamma$  happen at a much slower rate than the coupling  $g$ .

actions along  $z$ , while the Dicke-XXZ considers possible anisotropies among spin interactions.

Hybrid light-matter systems combine distinct components, spins, and photons, each with unique nature and demands, posing significant challenges to numerical simulations. Spins, as fermionic degrees of freedom, exhibit strong correlations that require many-body techniques [22–25] or quantum computational approaches [26–28]. Photons, on the other hand, belong to an unbounded bosonic Hilbert space with possibly large occupation numbers, where variational methods can be effective [29, 30]. Efficiently simulating many-body systems including strongly correlated fermionic and bosonic degrees of freedom requires hybrid techniques. Through a variational unitary transformation, such as the Lang-Firsov (LF) transformation [31, 32] and Jastrow wavefunctions [33, 34], the fermionic and bosonic degrees of freedom can be decoupled. By this means, the fermionic and spin degrees of freedom can be mapped to an exact solver applicable to strongly interacting systems, leading to self-consistent ground-state solutions, which has been verified in electron-phonon systems [35, 36]. In this work, we use a similar hybrid method to tackle the Dicke-Heisenberg Hamiltonian, enabling the investigation of the phases with strong spin interactions. We discover a striking difference between bare Dicke systems in which the competition between strong spin-spin and spin-photon interactions leads to a variety of quantum phenomena. In the Dicke-Ising model, we observed both first and second order phase transitions to the superradiant phase, while the Dicke-XXZ model supports a coexistence phase with both XY order and superradiance. In both systems, the mean photon number is enhanced compared to the Dicke model.

*The numerical approach.* The hybrid numerical approach adopted here leverages a non-Gaussian state (NGS) ansatz,  $|\psi\rangle = U_\lambda (|\psi_{\text{ph}}\rangle \otimes |\phi\rangle)$ , composed by a photonic state  $|\psi_{\text{ph}}\rangle$  and a many-body atomic state  $|\phi\rangle$  both dressed by a unitary entangling transformation  $U_\lambda$  [37, 38]. The photon state  $|\psi_{\text{ph}}\rangle$  can be expressed more generally but is often approximated by a Gaussian state  $|\text{GS}\rangle = U_{\text{GS}}|0\rangle$ , where  $|0\rangle$  is the vacuum and

$$U_{\text{GS}} = U_d U_S = \exp\left(i\mathbf{R}^T \boldsymbol{\sigma} \Delta_R\right) \exp\left(-\frac{i}{2}\mathbf{R}^T \boldsymbol{\xi} \mathbf{R}\right), \quad (3)$$

where  $\mathbf{R} = (x_1, x_2, \dots, x_n, p_1, p_2, \dots, p_n)^T \equiv (x, p)^T$  is the quadrature vector. This transformation is composed by two unitary operators, the displacement  $U_d$  and the squeezing  $U_S$ , where  $\Delta_R = (\Delta_x, \Delta_p)^T$  is the photon displacement vector and  $\boldsymbol{\xi}$  is the symmetric squeezing matrix. Due to the chosen form of spin-light interaction, we restrict  $\boldsymbol{\xi}$  to an anti-diagonal matrix. The vector  $\mathbf{R}$  transforms as  $U_{\text{GS}}^\dagger \mathbf{R} U_{\text{GS}} = \mathbf{S} \mathbf{R} + \Delta_R$  where  $\mathbf{S} = e^{\boldsymbol{\sigma} \boldsymbol{\xi}}$ . The variational NGS transformation  $U_\lambda$  introduces entanglement between photonic and atomic wavefunctions. Specifically, we adopt

$$U_\lambda = \exp\left\{i\frac{g'}{\omega} \sum_{i,j,\alpha} s_i^{(\alpha)} \lambda_{ij}^{(\alpha)} p_j\right\}, \quad (4)$$

analogous to previous studies in electron-phonon systems [35–37]. The parameters  $\{\lambda\}$  in  $U_\lambda$  control the spin-photon coupling and are determined self-consistently.

Through the variational wavefunctions, the group state of the Dicke-Heisenberg model can be obtained by minimizing the total energy  $\mathcal{E}(\Delta_R, \boldsymbol{\xi}, \lambda, |\phi\rangle) = \langle \psi | H | \psi \rangle$  in the variational wavefunction  $|\psi\rangle$ . There are two types of variational parameters to optimize, corresponding to the self-consistent iterations of two solvers: the variational parameters  $\Delta_R, \boldsymbol{\xi}, \lambda$  determine the NGS transformation and the photon state, optimized through the imaginary-time equations of motion; the many-body spin state  $|\phi\rangle$  is represented by the MPS variational states and the tensor coefficients are obtained with DMRG. In the latter step, all other variational parameters are fixed and  $|\phi\rangle$  can be obtained by solving the effective spin Hamiltonian  $H_{\text{eff}}(\Delta_R, \boldsymbol{\xi}, \lambda) = \langle \psi_{\text{ph}} | U_\lambda^\dagger H U_\lambda | \psi_{\text{ph}} \rangle$ . Additionally, for a single-mode cavity with Dicke-like spin-photon couplings,  $\lambda_{ij} = \delta_{ij} \hat{\mathbf{e}}_x \lambda$  is sufficient. These two iterations optimize all variational parameters in the wavefunction in a self-consistent manner, ensuring the energy decrease.

We start with the conventional Dicke model without spin-spin interactions ( $J_\alpha = 0$ ), benchmarking the validity and efficiency of the hybrid method against established results. Focusing on the key observables, namely average energy, photon number, and magnetization, we observe from our hybrid numerical method the renowned superradiant phase transition at  $g_c = \sqrt{\omega\varepsilon}/2$  [see Figs. 2(a) and (b)] for  $N = 200$ . Magnetization

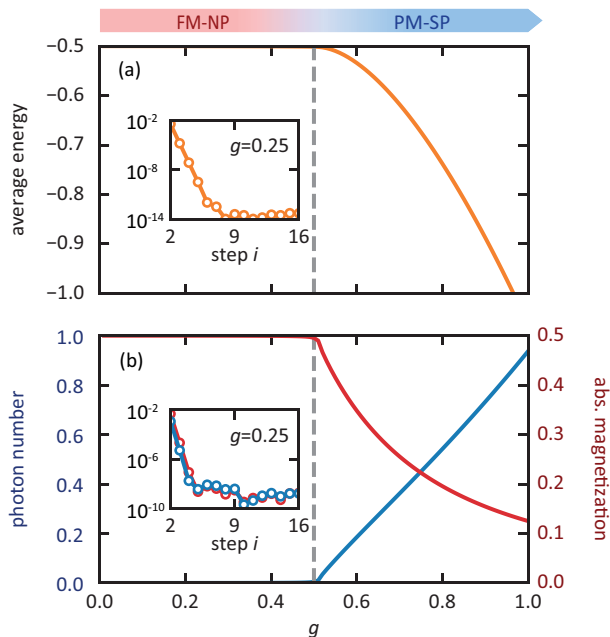


FIG. 2. Benchmarking the Hybrid Method with the Dicke Model. Key ground-state observables are shown: (a) average energy, (b) mean photon number, and absolute magnetization for  $N = 200$ . The inset shows the quick convergence at  $g = 0.25$  via  $O[i+1] - O[i]$ , stabilizing below  $10^{-12}$  for energy and  $10^{-8}$  for photon number and magnetization.

$M_z = \sum_i \langle s_i^z \rangle / N$  and mean photon number  $\langle n \rangle / N$  [39] shift from  $M_z = -1/2, \langle n \rangle / N = 0$  in the normal phase to  $M_z = 0, \langle n \rangle / N > 0$  in the superradiant phase. In the normal phase, the phase of vanishing photons, the mean photon number should not grow with the system size  $N$ , while in the superradiant phase it scales linearly with the number of particles  $\langle n \rangle \propto N$ , meaning that  $\langle n \rangle / N \approx 0$  in the normal phase, as observed. Additionally, for an increasingly large  $N$ , the ground state approaches a fully coherent state, represented by  $\xi = \lambda = 0$  and  $|\phi\rangle = \exp(-i\phi s^y) |j, -j\rangle$ . Numerical results converge rapidly to this coherent state, even for a large  $N = 200$ , as shown in the inset of Fig. 2. These results are consistent with mean-field theory predictions [21], where the ground-state energy, defined as  $E_0 = (\mathcal{E}_{\min} - \omega/2)/N$ , equals  $-\varepsilon/2$  for the ferromagnetic-normal phase ( $g \leq g_c$ ) and  $-(g^4 + g_c^4)/\omega g^2$  for the paramagnetic-superradiant phase ( $g \geq g_c$ ), as shown in Fig. 2(a).

*The Dicke-Ising model.* Building on this benchmark, we turn on the spin-spin interactions and investigate the phase diagram of the Dicke-Ising model [38]. This competition directly impacts the superradiant properties of the system and challenges traditional methods, as these interactions introduce nontrivial correlations. To isolate the effect of Ising-like couplings, we set  $J_x = J_y = 0$  and  $J_z = 4J$ . The simulations reveal that spin-spin interactions significantly modify the phase diagram, where we observe three distinct phases: ferromagnetic-

normal (FM-NP), antiferromagnetic-normal (AFM-NP), and paramagnetic-superradiant (PM-SP). The Dicke model critical coupling is modified, as we explain in the following, and we obtain  $J_c = -\varepsilon/4$  for  $g = 0$ , which defines the *ferromagnetic* ( $J > J_c$ ) and *antiferromagnetic* ( $J < J_c$ ) parameter regimes. Indeed, these two types of interactions have distinct physical origins: in systems governed by Hund's coupling where intra-atomic exchange favors parallel spin alignment the effective interaction is ferromagnetic, while in systems where the interaction arises from superexchange processes (as in Hubbard models), the coupling is inherently antiferromagnetic [40].

As the atom-photon coupling  $g$  increases, the Dicke-Ising model transitions through distinct phases, shaped by the interplay between cavity-induced dynamics and spin-spin interactions. For  $J > J_c$ , the system undergoes a continuous phase transition from FM-NP to PM-SP, characterized by the emergence of superradiance ( $\langle n \rangle / N > 0$ ) and lack of spin order at the critical coupling  $g_c(J) = g_c \sqrt{1 - J/J_c}$ . This behavior, shown in Fig. 3(b), demonstrates the robustness of the second-order transition and highlights the evolution of the symmetry-breaking mechanism of the Dicke model under ferromagnetic interactions. Our numerical simulations reveal a shift in energy within the FM-NP phase, while in the  $g \gg J$  limit (deep in the PM-SP phase), the energy agrees with the Dicke model ( $J = 0$ ). Furthermore, the spin correlations  $\langle s_i^z s_{i+r}^z \rangle$  always measured in the bulk ( $i = N/4 - 1$  and  $r < N/2$ ) equal to  $1/4$  confirm the presence of spin order in the FM-NP phase and its absence in the PM-SP phase. Interestingly, prior work by Rohn et al. [41] used an exact diagonalization approach to study the system, requiring Hilbert space truncation and simulations limited to small sizes. By comparing their numerical results with the well-known limiting cases for the energy of the system ( $E_0 = -J$  for  $g \ll g_c$  and  $E_0 = -g^2/\omega$  for  $g \gg g_c$ ), they predicted a first-order phase transition. However, our analysis of relevant observables in Fig. 3(b) reveals that the FM-NP to PM-SP transition remains second order despite the shift in critical coupling caused by the ferromagnetic interaction.

In the antiferromagnetic regime ( $J < J_c$ ), the system shows abrupt, discontinuous changes in relevant observables, indicating a first-order phase transition from the antiferromagnetic-normal (AFM-NP) to PM-SP phases—this is even more evidenced in the thermodynamic limit given by the coherent state limit. Unlike the ferromagnetic case, where the transition is of second order, this change reflects a shift in the system's fundamental behavior as the value of  $J$  is modified. The degeneracy of the AFM ground state persists until the phase transition point, as the external field alone is insufficient to break the symmetry in the AFM phase. Additionally, the persistence of long-range AFM order is confirmed through the staggered spin correlations  $\langle (-1)^r s_i^z s_{i+r}^z \rangle = -1/4$  in

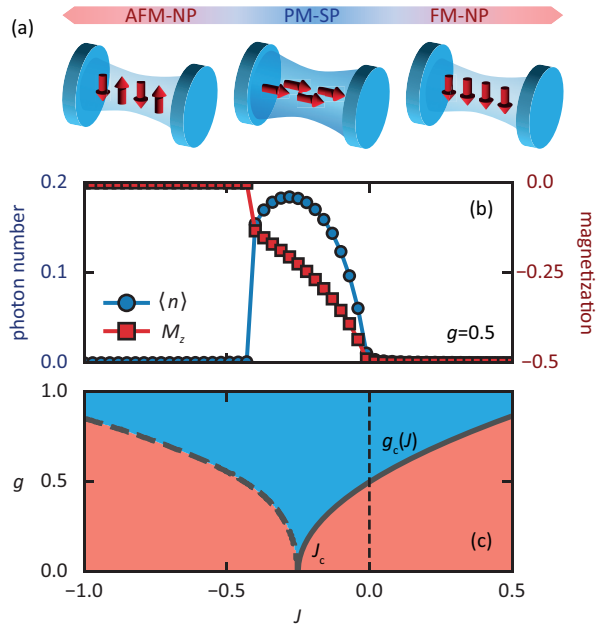


FIG. 3. (a) Spin-photon phases cartoon. (b) The behavior of the magnetization and mean photon number in the three distinct phases for  $g = 0.5$  and  $N = 100$  is shown. One can observe that the FM-NP to PM-SP phase transition is of second order while the AFM-NP to PM-SP is of first order, where the first derivative of the order parameters is infinite. (c) Phase diagram of the Dicke-Ising model. Lines separate the normal-superradiant phases, where the spin system goes from ordered to a paramagnetic phase. Solid (dashed) curves depict second(first)-order transitions. Horizontal black dashed line represents the bare Dicke model. The FM-NP to PM-SP transition line matches the analytical result.

the bulk. These results emphasize the role of AFM interactions in altering the nature of the phase transition. Distinct from a recent mean-field study indicating co-existing AFM spin order and photon superradiance [42], our hybrid numerical simulations identify the many-body state with lower energy by treat the spin states exactly.

The phase diagram in Fig. 3(c) reveals the how the competition between spin-photon and spin-spin interactions leads to the distinct phases reported. Solid and dashed lines represent second and first order transitions, respectively. Interestingly, the mean photon number grows larger when spin-spin interactions are present. As shown in Fig. 3(b), for  $g = 0.5$ , which equals the Dicke critical coupling, the photon number ranges from zero to  $\approx 0.2$ , while the Dicke superradiance only starts to build up for a larger coupling strength. This can be experimentally beneficial for superradiant state design: tuning the experimental parameters can lead to an optimal spin-spin interaction strength that maximizes the mean number of photons.

*Dicke-XXZ model.* Beyond isotropic spin-spin couplings, many experimental systems naturally exhibit

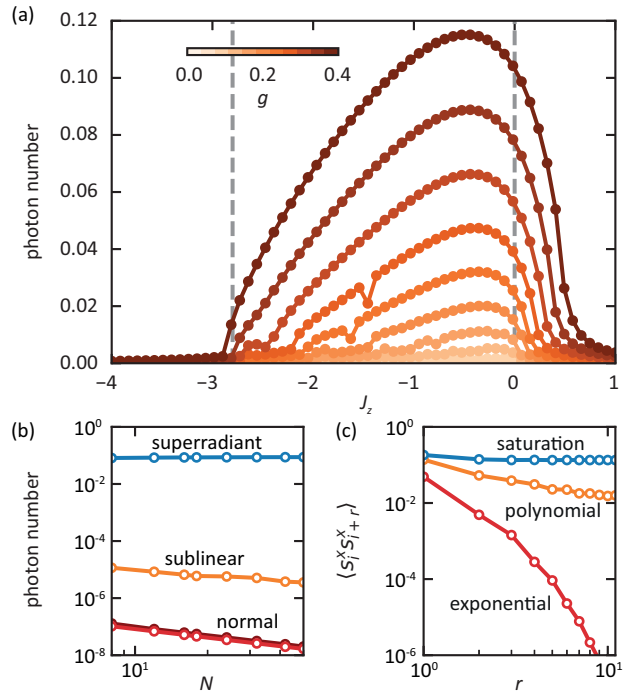


FIG. 4. Phase characterization of the Dicke-XXZ model. (a) The mean photon number,  $\langle n \rangle / N$ , as a function of  $J_z$  for increasing coupling strength  $g$ , highlighting the sensitivity of the intermediate regime to the atom-light interaction for  $N = 24$ . (b) Scaling of  $\langle n \rangle / N$  with system size  $N \in [8, 50]$  in all regimes. The FM/AFM-normal phases exhibit a  $\langle n \rangle / N \propto 1/N$  decay (dark/light red:  $g = 0.01$ ,  $J_z = -10, 10$ ). The superradiant phase indicates  $\langle n \rangle \propto N$  (blue:  $g = 0.4$ ,  $J_z = -1.6$ ), while in the regime of moderate negative  $J_z$  a sublinear scaling emerges (orange:  $g = 0.01$ ,  $J_z = -1.6$ ). (c) The xx spin-spin correlation  $\langle s_i^x s_{i+r}^x \rangle$  as a function of distance  $r$  for  $N = 24$ . The FM/AFM-NP phases exhibit exponential decay (red:  $J_z = -5$ ,  $g = 0.01$ ), while the superradiant phase supports long-range order (blue:  $J_z = -1.6$ ,  $g = 0.4$ ). In the intermediate regime, correlations follow a polynomial/power-law decay, characteristic of the quasi-long-range order of the XY phase (orange:  $J_z = -1.6$ ,  $g = 0.04$ ).

anisotropic interactions due to directional dipolar couplings and tunneling processes [43, 44]. Building on our Dicke and Dicke-Ising results, we introduce the Dicke-XXZ model, where  $J_x = J_y = 1$  and  $J_z$  is a tunable anisotropy parameter. This extension enables us to investigate how anisotropic couplings further influence the emergence and stability of quantum phases, including photon-mediated magnetic orders.

We numerically find distinct phases in the Dicke-XXZ model, including FM/AFM-NP phases that align with the Dicke-Ising model, but Néel order and, consequently, first-order AFM-PM phase transitions are not observed. These ordered phases are destabilized by the atom-photon coupling strength in a similar fashion compared to the Dicke-Ising model, i.e. superradiance destroys the spin order around the critical QPT points at

$J_c^{FM} = 0$  and  $J_c^{AFM} \approx -2.8$  [45] ( $g = 0$ ) and broadens up for an increasing  $g$  [see Fig.4(a)]. Additionally, the staggered spin correlations  $\langle (-1)^r s_i^z s_{i+r}^z \rangle$ , clearly show that the AFM order is achieved. In contrast, the spin correlations along the x-direction  $\langle s_i^x s_{i+r}^x \rangle$  decay exponentially with  $r$ , leading to short-range fluctuations [see Fig.4(c)].

For moderate  $J_c^{AFM} < J_z < J_c^{FM}$  between the phases mentioned above, the scenario is completely different. There is always a non-vanishing mean photon number  $\langle n \rangle / N$  for a non-zero coupling strength  $g$ . In this regime, the transverse cavity field couples directly to the in-plane spin components, it allows the superradiant photon population to remain high even as XY order is suppressed. When compared to the FM/AFM parameter regions, we observe that the mean photon number in the PM-SP phase is much larger within the XY region, reflecting the enhanced sensitivity of spin fluctuations to the atom-light interaction [see Fig. 4(a)] To confirm that this phase of non-vanishing photons is a superradiant phase coexisting with the XY order, we calculate the  $\langle n \rangle$  scaling with  $n$  and the spin-spin correlations. We show in Fig. 4(b) the scaled mean photon number  $\langle n \rangle / N$  as a function of  $N$  for some exemplary values of  $g$  and  $J_z$ . In the FM/AFM-NP phases, where  $g$  is small and  $|J_z|$  large, the result is a power law decay  $\approx 1/N$ , while in the superradiant phase, where  $g$  is comparatively large, the result is an almost flat line, as expected. However, for a moderate negative  $J_z$  and  $g \neq 0$ , we obtain a power law decay of the form  $\langle n \rangle / N \propto N^{-\alpha}$  with  $0 < \alpha < 1$ , corresponding to a sublinear scaling  $\langle n \rangle \propto N^{1-\alpha}$ . That is, we observe a superradiant phase with additional magnetic fluctuations encoded in  $\alpha$ , which decay continuously towards  $\alpha = 0$  for increasing  $g$ . In Fig. 4(c), we observe that in this sublinear scaling regime,  $\langle s_i^x s_{i+r}^x \rangle$  follows a power-law decay, characteristic of the quasi-long-range order of the XY phase. In contrast, the correlations decay exponentially in the FM/AFM-NP phases, while long-range order is established in the superradiant phase. Increasing  $g$ , the superradiant scaling is achieved and the XY phase is completely suppressed by the paramagnetic phase.

In conclusion, we systematically studied the impact of spin-spin interactions to the phases of the Dicke model in a one-dimensional chain. Using a hybrid many-body method which captures both the strong coupling and strong correlations, we found that the Ising-type interactions shift the superradiant phase boundary, exhibiting both first- and second-order transitions, and notably enhance the mean photon number in the PM-SP phase compared to the conventional Dicke model. When considering anisotropic interactions representing tunneling effects, our results revealed a complex interplay between anisotropy and photon coupling. A unique intermediate phase emerges from anisotropic interactions, where the XY spin order and sublinearly scaling average phonon number coexist. These results reveal that incorporating

spin-spin interactions not only dramatically enhances the superradiant response, but also critically tunes the phase transitions, providing a framework for future experiments and applications in engineered light-matter quantum devices.

*Acknowledgments.* This work was supported by the Polish National Agency for Academic Exchange (NAWA) via the Polish Returns 2019 program. We gratefully acknowledge Polish high-performance computing infrastructure PLGrid (HPC Center: ACK Cyfronet AGH) for providing computer facilities and support within computational grant no. PLG/2024/017478. Y.W. acknowledges the support by the U.S. Department of Energy, Office of Science, Basic Energy Sciences, under Early Career Award No. DE-SC0024524.

\* [jpiedromend@gmail.com](mailto:jpiedromend@gmail.com)

† [Krzysztof.Jachymski@fuw.edu.pl](mailto:Krzysztof.Jachymski@fuw.edu.pl)

‡ [yao.wang@emory.edu](mailto:yao.wang@emory.edu)

- [1] J. P. Dowling and G. J. Milburn, Quantum technology: the second quantum revolution, Philosophical Transactions of the Royal Society of London. Series A: Mathematical, Physical and Engineering Sciences **361**, 1655 (2003).
- [2] S. Julià-Farré, T. Salamon, A. Riera, M. N. Bera, and M. Lewenstein, Bounds on the capacity and power of quantum batteries, Physical Review Research **2**, 023113 (2020).
- [3] B. Julsgaard, J. Sherson, J. I. Cirac, J. Fiurášek, and E. S. Polzik, Experimental demonstration of quantum memory for light, Nature **432**, 482 (2004).
- [4] M. Mitrano, A. Cantaluppi, D. Nicoletti, S. Kaiser, A. Perucchi, S. Lupi, P. Di Pietro, D. Pontiroli, M. Riccò, S. R. Clark, *et al.*, Possible light-induced superconductivity in  $\text{k3c60}$  at high temperature, Nature **530**, 461 (2016).
- [5] H. Ritsch, P. Domokos, F. Brennecke, and T. Esslinger, Cold atoms in cavity-generated dynamical optical potentials, *Rev. Mod. Phys.* **85**, 553 (2013).
- [6] D. De Bernardis, T. Jaako, and P. Rabl, Cavity quantum electrodynamics in the nonperturbative regime, *Phys. Rev. A* **97**, 043820 (2018).
- [7] A. Safavi-Naini, R. J. Lewis-Swan, J. G. Bohnet, M. Gärttner, K. A. Gilmore, J. E. Jordan, J. Cohn, J. K. Freericks, A. M. Rey, and J. J. Bollinger, Verification of a many-ion simulator of the dicke model through slow quenches across a phase transition, *Phys. Rev. Lett.* **121**, 040503 (2018).
- [8] G. Findik, M. Biliroglu, D. Seyitliyev, J. Mendes, A. Barrette, H. Ardekani, L. Lei, Q. Dong, F. So, and K. Gundogdu, High-temperature superfluorescence in methyl ammonium lead iodide, Nature Photonics **15**, 676 (2021).
- [9] K. Baumann, C. Guerlin, F. Brennecke, and T. Esslinger, Dicke quantum phase transition with a superfluid gas in an optical cavity, nature **464**, 1301 (2010).
- [10] E. J. Davis, A. Periwal, E. S. Cooper, G. Bentsen, S. J. Evered, K. Van Kirk, and M. H. Schleier-Smith, Protecting spin coherence in a tunable heisenberg model, *Phys. Rev. Lett.* **125**, 060402 (2020).

- [11] A. Periwal, E. S. Cooper, P. Kunkel, J. F. Wienand, E. J. Davis, and M. Schleier-Smith, Programmable interactions and emergent geometry in an array of atom clouds, *Nature* **600**, 630 (2021).
- [12] D. Ferraro, M. Campisi, G. M. Andolina, V. Pellegrini, and M. Polini, High-power collective charging of a solid-state quantum battery, *Phys. Rev. Lett.* **120**, 117702 (2018).
- [13] J. Q. Quach, K. E. McGhee, L. Ganzer, D. M. Rouse, B. W. Lovett, E. M. Gauger, J. Keeling, G. Cerullo, D. G. Lidzey, and T. Virgili, Superabsorption in an organic microcavity: Toward a quantum battery, *Science advances* **8**, eabk3160 (2022).
- [14] F.-Q. Dou, H. Zhou, and J.-A. Sun, Cavity heisenberg-spin-chain quantum battery, *Phys. Rev. A* **106**, 032212 (2022).
- [15] R. F. Ribeiro, L. A. Martínez-Martínez, M. Du, J. Campos-Gonzalez-Angulo, and J. Yuen-Zhou, Polariton chemistry: controlling molecular dynamics with optical cavities, *Chemical science* **9**, 6325 (2018).
- [16] P. Strack and S. Sachdev, Dicke quantum spin glass of atoms and photons, *Phys. Rev. Lett.* **107**, 277202 (2011).
- [17] S. P. Kelly, A. M. Rey, and J. Marino, Effect of active photons on dynamical frustration in cavity qed, *Phys. Rev. Lett.* **126**, 133603 (2021).
- [18] S. J. Masson, M. D. Barrett, and S. Parkins, Cavity qed engineering of spin dynamics and squeezing in a spinor gas, *Phys. Rev. Lett.* **119**, 213601 (2017).
- [19] A. Niezgoda, M. Panfil, and J. Chwedeńczuk, Quantum correlations in spin chains, *Phys. Rev. A* **102**, 042206 (2020).
- [20] M. Płodzień, T. Wasak, E. Witkowska, M. Lewenstein, and J. Chwedeńczuk, Generation of scalable many-body bell correlations in spin chains with short-range two-body interactions, *Phys. Rev. Res.* **6**, 023050 (2024).
- [21] P. Kirton, M. M. Roses, J. Keeling, and E. G. Dalla Torre, Introduction to the dicke model: From equilibrium to nonequilibrium, and vice versa, *Advanced Quantum Technologies* **2**, 1800043 (2019).
- [22] S. R. White, Density matrix formulation for quantum renormalization groups, *Phys. Rev. Lett.* **69**, 2863 (1992).
- [23] S. R. White, Density-matrix algorithms for quantum renormalization groups, *Phys. Rev. B* **48**, 10345 (1993).
- [24] A. Wietek and A. M. Läuchli, Sublattice coding algorithm and distributed memory parallelization for large-scale exact diagonalizations of quantum many-body systems, *Phys. Rev. E* **98**, 033309 (2018).
- [25] A. M. Läuchli, J. Sudan, and R. Moessner,  $s = \frac{1}{2}$  kagome heisenberg antiferromagnet revisited, *Phys. Rev. B* **100**, 155142 (2019).
- [26] S. J. Evered, D. Bluvstein, M. Kalinowski, S. Ebadi, T. Manovitz, H. Zhou, S. H. Li, A. A. Geim, T. T. Wang, N. Maskara, *et al.*, High-fidelity parallel entangling gates on a neutral-atom quantum computer, *Nature* **622**, 268 (2023).
- [27] I. Cong, H. Levine, A. Keesling, D. Bluvstein, S.-T. Wang, and M. D. Lukin, Hardware-efficient, fault-tolerant quantum computation with rydberg atoms, *Phys. Rev. X* **12**, 021049 (2022).
- [28] A. Browaeys and T. Lahaye, Many-body physics with individually controlled rydberg atoms, *Nature Physics* **16**, 132 (2020).
- [29] T. Guaita, L. Hackl, T. Shi, C. Hubig, E. Demler, and J. I. Cirac, Gaussian time-dependent variational principle for the bose-hubbard model, *Phys. Rev. B* **100**, 094529 (2019).
- [30] A. Christianen, J. I. Cirac, and R. Schmidt, Bose polaron and the efimov effect: A gaussian-state approach, *Phys. Rev. A* **105**, 053302 (2022).
- [31] H. Fehske, H. Röder, G. Wellein, and A. Mitrakis, Hole-polaron formation in the two-dimensional holstein t-j model: A variational lanczos study, *Phys. Rev. B* **51**, 16582 (1995).
- [32] Y. Takada and A. Chatterjee, Possibility of a metallic phase in the charge-density-wave–spin-density-wave crossover region in the one-dimensional hubbard-holstein model at half filling, *Physical Review B* **67**, 081102 (2003).
- [33] S. Karakuzu, L. F. Tocchio, S. Sorella, and F. Becca, Superconductivity, charge-density waves, antiferromagnetism, and phase separation in the hubbard-holstein model, *Phys. Rev. B* **96**, 205145 (2017).
- [34] T. Ohgoe and M. Imada, Competition among superconducting, antiferromagnetic, and charge orders with intervention by phase separation in the 2d holstein-hubbard model, *Phys. Rev. Lett.* **119**, 197001 (2017).
- [35] Y. Wang, I. Esterlis, T. Shi, J. I. Cirac, and E. Demler, Zero-temperature phases of the two-dimensional hubbard-holstein model: A non-gaussian exact diagonalization study, *Phys. Rev. Res.* **2**, 043258 (2020).
- [36] Y. Wang, T. Shi, and C.-C. Chen, Fluctuating nature of light-enhanced d-wave superconductivity: a time-dependent variational non-gaussian exact diagonalization study, *Physical Review X* **11**, 041028 (2021).
- [37] T. Shi, E. Demler, and J. I. Cirac, Variational study of fermionic and bosonic systems with non-gaussian states: Theory and applications, *Annals of Physics* **390**, 245 (2018).
- [38] J. P. Mendonça, Y. Wang, K. Jachymski, in preparation.
- [39] We refer to observables as their value per particle, i.e., divided by  $N$ . Their counterparts without this normalization, representing the total quantity, are explicitly referred to as “total (observable name)”.
- [40] D. C. Mattis, Ferromagnetism and spin waves in the band theory, *Phys. Rev.* **132**, 2521 (1963).
- [41] J. Rohn, M. Hörmann, C. Genes, and K. P. Schmidt, Ising model in a light-induced quantized transverse field, *Phys. Rev. Res.* **2**, 023131 (2020).
- [42] Y. Zhang, L. Yu, J.-Q. Liang, G. Chen, S. Jia, and F. Nori, Quantum phases in circuit qed with a superconducting qubit array, *Scientific Reports* **4**, 4083 (2014).
- [43] A. de Paz, A. Sharma, A. Chotia, E. Maréchal, J. H. Huckans, P. Pedri, L. Santos, O. Gorceix, L. Vernac, and B. Laburthe-Tolra, Nonequilibrium quantum magnetism in a dipolar lattice gas, *Phys. Rev. Lett.* **111**, 185305 (2013).
- [44] A. Micheli, G. K. Brennen, and P. Zoller, A toolbox for lattice-spin models with polar molecules, *Nature Physics* **2**, 341 (2006).
- [45] L. Justino and T. R. de Oliveira, Bell inequalities and entanglement at quantum phase transitions in the  $XXZ$  model, *Phys. Rev. A* **85**, 052128 (2012).